WATER RESOURCES RESEARCH, VOL. 36, NO. 2, PAGES 571–583, FEBRUARY 2000

When do logs move in rivers?

Christian A. Braudrick
Department of Geosciences, Oregon State University, Corvallis

Gordon E. Grant
Pacific Northwest Research Station, U.S. Forest Service, Cornallis, Oregon

Abstract. Large woody debris is an integral component of forested, fluvial systems throughout the world, yet we know little about hydraulic thresholds for movement and transport of logs. We developed theoretical models of entrainment and performed flume experiments to examine thresholds for wood movement in streams. Both the model and the experiments indicate that log entrainment is primarily a function of the piece angle relative to flow direction, whether or not the log had a rootwad, the density of the log, and the piece diameter. Stability increased if the pieces had rootwads or were rotated parallel to flow. Although previously reported as the most important factor in piece stability, piece length did not significantly affect the threshold of movement in our experiments or our physically based model, for logs shorter than channel width. These physically based models offer a first-order approach to evaluating the stability of either naturally derived woody debris or material deliberately introduced to streams for various management objectives.

1. Introduction

Advances in our understanding of the ecologic and geomorphic roles of large woody debris (LWD) in streams over the last 20 years [e.g., *Harmon et al.,* 1986; *Sedell and Froggatt*, 1984; *Lisle,* 1995; *Montgomery et al.,* 19961 have dramatically changed perceptions of wood in some parts of the world, such as the U.S. Pacific Northwest. Wood in streams is no longer viewed as an unsightly barrier to fish migration that needs to be removed but an integral part of aquatic ecosystems that needs to be replenished. To this end, millions of dollars are spent each year protecting riparian forests and returning wood to streams in an effort to restore aquatic habitat and geomorphic function. At the same time wood in streams continues to be seen as a natural hazard increasing flood impacts in densely populated areas (e.g., Japan, Europe, and parts of the United States) and is actively removed. However, much of this recent interest in the ecologic, geomorphic, and potential hazard effects of wood in streams has not been based on sound geotechnical analysis. In order to assess the potential interaction between wood and both ecologic and geologic systems, we need to better understand the dynamics of wood movement within streams.

At present, we have no quantitative models of hydraulic conditions at which wood movement occurs and cannot therefore assess the relative stability of either natural or artificially introduced pieces. Since LWD tends to move during large floods, safety and logistical constraints make field measurements difficult. As a result there is little direct observation and measurement of conditions of wood entrainment and transport. Similar problems faced researchers studying sediment transport in the first half of this century, who used physical models and flume experiments to study aspects of transport dynamics that were difficult to observe in the field. Such models and experiments have contributed greatly to our present knowledge of sediment transport but have received little attention as a tool to improve our understanding of LWD movement in streams.

In this paper we report the results of a series of flume experiments conducted at the St. Anthony Falls Hydraulic Laboratory, in which we modeled entrainment of individual logs in streams. These experiments were designed to test a simple entrainment model based on the balance of forces exerted on individual logs by moving water. We recognize that the interaction among multiple pieces can play an important role in both entrainment and deposition, as stationary pieces can be entrained when they are struck by moving pieces or by diversion of flow from other stationary pieces *[Braudnck et al.,* 1997]. The shape of the bank and presence of riparian vegetation can also influence movement thresholds of wood by either elevating the piece off the bed or obstructing piece movement. Because thresholds of movement have not previously been quantified, however, we decided to focus on the simpler case of movement of individual logs without considering bank or vegetation effects.

2. Previous Research

Previous field studies on fluvial transport of LWD inferred transport relations from mapped temporal changes in LWD distribution in first- to fifth-order streams [*Toews and Moore,* 1982; *Hogan,* 1987; *Lienkaemper and Swanson,* 1987; *Bilby and Ward,* 1989; *Gregory,* 1991; *Nakamura and Swanson,* 1994; *Young,* 1994]. These studies showed that smaller logs move farther than larger ones *[Lienkaemper and Swanson,* 1987; *Young,* 19941, frequency of log movement increases with increasing stream size *[Bilby,* 1985; *Lienkaemper and Swanson,* 1987; *Bilby and Ward,* 1989, 19911, and most mobile pieces are shorter than bankfull width *[Nakamura and Swanson,* 19941. Taken together, these studies suggest that piece length relative

Paper number 1999WR900290.
0043-1397/00/1999WR900290$09.00

to average channel width ($L_{\log}/w_{av}$) is a good first-order approximation of the likelihood of piece movement. Pieces tend to be stable when piece length is greater than one-half bankfull width in large rivers *[Abbe et al.*, 1993] or greater than bankfull width in smaller rivers *[Lienkaemper and Swanson*, 1987]. However, we lack models that predict how piece length affects stability over a range of stream sizes.

Other factors besides length can affect frequency of piece transport. Rootwads can inhibit LWD movement by anchoring pieces to the bed, increasing drag and thereby decreasing mobility *[Abbe und Montgomery*, 1996]. Piece diameter strongly influences the depth of flow required to entrain and transport logs *[Bilby and Ward*, 1989; *Abbe et al.*, 1993]. Pieces also tend to be stable when greater than half their length is outside the channel area because less of the piece is exposed to flow *[Lienkaemper and Swanson*, 1987].

There has been recent interest in physically based quantification of wood in streams that use both flume and field experiments to examine either the hydraulic role of wood or wood dynamics [e.g., *Zshikawa*, 1989; *Gippel et al.*, 1996; *Braudrick et al.*, 1998; *Abbe et al.*, 1998]. However, we still lack a general model for wood movement in streams.

3. Theoretical Background

We consider wood entrainment in relation to a force balance model acting on wood in streams. Because models of wood entrainment in streams are rare, we decided to model the simple case of a right-circular cylindrical log in a uniform flow field, lying on a smooth, immobile planar stream bed. We also assume that the cylinder moves initially by sliding, although the initial motion in nature is typically more complex involving pivoting and sliding. Neglecting these effects, the piece moves when its downstream components (gravitational force and drag force) and upstream components (frictional force) are balanced. We also assume that all forces are body forces and act on the center of mass. We do not include the lift force, a common component of sediment transport equations, because logs are often not submerged, which makes the lift force negligible.

The gravitational force (F_{gravity}) acting on the log is equal to the effective weight of the log (W_{eff} = weight force minus buoyant force) in the downstream direction and is equal to

$$F_{\text{gravity}} = -W_{\text{eff}} \sin \alpha = -\left(g\rho_{\log} L_{\log} \frac{\pi D_{\log}^2}{4} - g\rho_w L_{\log} A_{\text{sub}} \right) \sin \alpha, \quad (1)$$

where $L_{\log}$ is the piece length, $\rho_{\log}$ and ρ_w are the densities of wood and water, respectively, $D_{\log}$ is piece diameter, α is the bed angle in the flow-parallel plane (equal to the bed slope at low values of α), g is gravity, and A_{sub} is the submerged area of the log perpendicular to piece length exposed to drag (Figure 1).

The friction force (F_{friction}) on the log acts in the upstream direction and is equal to the normal force ($F_n = F_{\text{weff}} \cos \alpha$) acting on the log times the coefficient of friction between the wood and the bed:

$$F_{\text{friction}} = F_n \mu_{\text{bed}} = \left(g\rho_{\log} L_{\log} \frac{\pi D_{\log}^2}{4} - g\rho_w L_{\log} A_{\text{sub}} \right) \mu_{\text{bed}} \cos \alpha, \quad (2)$$

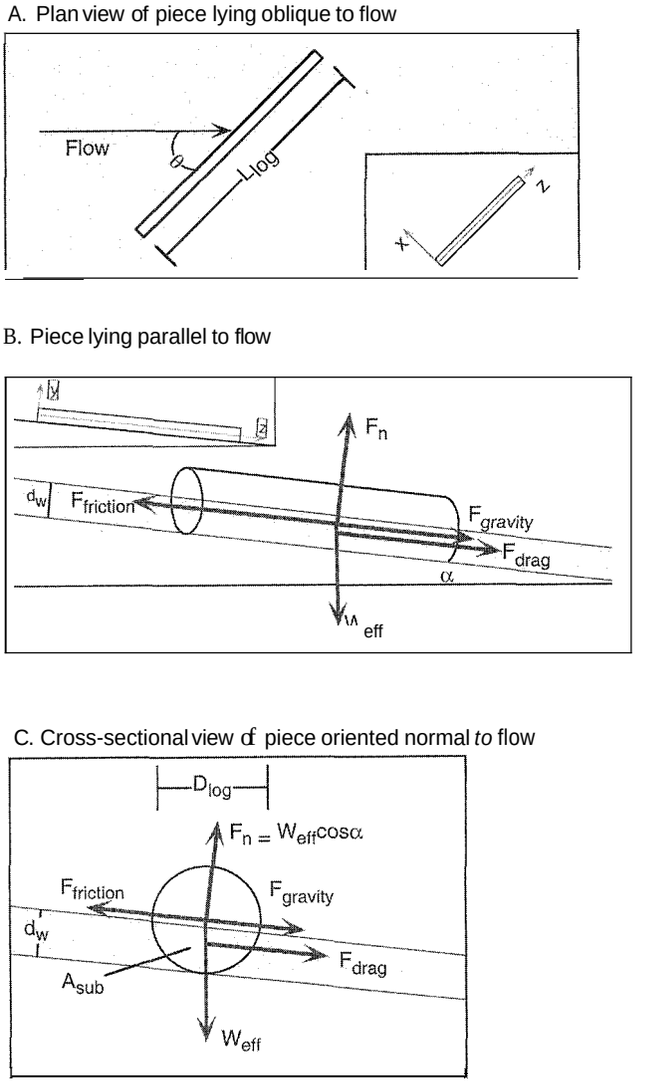

Figure 1. Schematic and body-force diagrams of some of the components of the force balance acting on a log without a rootwad. All body force vectors are schematic, and the coordinate system shown in the insets was used to calculate piece volume not for the force balance.

where μ_{bed} is the coefficient of friction between the wood and bed (Figure 1). The drag force (F_{drag}) is the downstream drag exerted on the log by moving water and is equal to

$$F_{\text{drag}} = -\frac{U^2}{2} \rho_w C_d (L_{\log} d_w \sin \theta + A_{\text{sub}} \cos \theta), \quad (3)$$

where U is the water velocity, d, is flow depth, C_d is the drag coefficient of the wood in water, and θ is the angle of the piece relative to flow, with $\theta = 0°$ when the log is parallel to flow (Figure 1).

Combining these three equations gives the force balance at incipient motion for a right circular cylinder on a smooth, planar bed: $F_{\text{friction}} + F_{\text{gravity}} = F_{\text{drag}}$ or

$$\left(g\rho_{\log} L_{\log} \frac{\pi D_{\log}^2}{4} - g\rho_w L_{\log} A_{\text{sub}} \right) (\mu_{\text{bed}} \cos \alpha - \sin \alpha) = \frac{U^2}{2} \rho_w C_d (L_{\log} d_w \sin \theta + A_{\text{sub}} \cos \theta). \quad (4)$$

A_{sub} is a function of water depth and piece diameter equal to

$$A_{sub} = 2 \int_{r}^{d_w - r} \int_{0}^{\sqrt{r^2 - y^2}} dx\, dy \tag{5}$$

which for a right-circular cylinder resolves to

$$A_{sub} = \left\{ 2 \cos^{-1}\left(1 - \frac{2d_w}{D_{log}} \right) - \sin\left[2 \cos^{-1}\left(1 - \frac{2d_w}{D_{log}} \right) \right] \right\} \frac{D_{log}^2}{8}. \tag{6}$$

Equation (4) indicates that entrainment is a function of four piece characteristics, length, density, diameter, and orientation, and three hydraulic characteristics, slope, water velocity, and channel depth (Figure 1). If the piece is oriented normal to flow ($\theta = 90°$), A_{sub} Cos $\theta = 0$, which cancels out piece length from the equation. In essence, this is because both the left-hand and right-hand sides of (4) increase linearly with increased piece length, when the log is normal to flow. However, piece length should affect stability at other orientations.

If a rootwad is attached to a log, the piece is elevated off the bed a certain height depending on the ratio of piece length to rootwad diameter, provided that the rootwad is not buried in a scour hole. This effectively reduces the buoyant force and the portion of the log exposed to flow. If we model rootwads as disks on the end of cylinders (Figure 2) and make the same assumptions as in (4), the force balance acting on a log with a rootwad can be calculated in a similar manner by equating the upstream (frictional force) and downstream (weight and drag forces) components (Figure 2). The gravitational force of a piece with a rootwad is equal to the weight of the log minus its buoyant force:

$$F_{gravity} = -\left[g\rho_{log}\left(L_{log} \frac{\pi D_{log}^2}{4} + V_2 \right) \right] \sin a, \tag{7}$$

where V_{rw} is the rootwad volume and V_1 and V_2 are the submerged volumes of the bole and rootwad, respectively (Figure 2). The frictional force of a log with a disk shaped rootwad is

$$F_{friction} = \left[g\rho_{log}\left(L_{log} \frac{\pi D_{log}^2}{4} V_{rw} \right) - g\rho_w(V_1 + V_2) \right] \mu_{bed} \cos \alpha. \tag{8}$$

The drag force acting on a log with a rootwad in a uniform flow field is

$$F_{drag} = -\frac{U^2}{2} \rho_w C_d [(A_1 + A_2) \sin \theta + A_3 \cos \theta], \tag{9}$$

where A_1 and A_2 are the submerged areas of the bole and rootwad in the cross section, respectively; A_3 is the submerged area of the rootwad perpendicular to piece length (Figure 2).

Adding these equations gives the force balance for a log with a disk-shaped rootwad in a river:

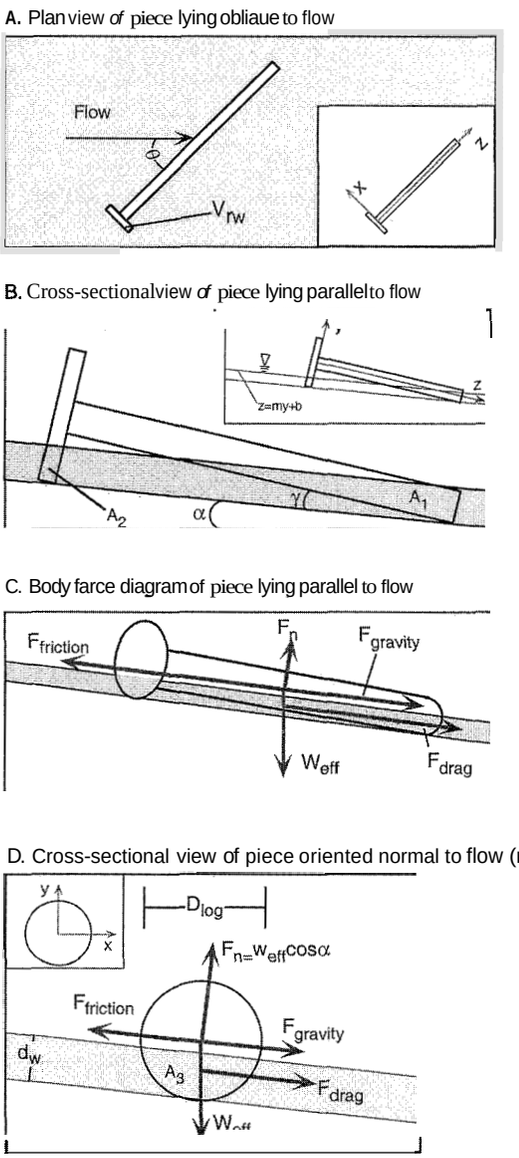

Figure 2. Schematic and body-force diagrams of some of the components of the force balance acting on a log with a rootwad. All body force vectors are schematic, and the coordinate system shown in the insets was used to calculate piece volume not for the force balance.

$$\left[g\rho_{log}\left(L_{log} \frac{\pi D_{log}^2}{4} + V_{rw} \right) - g\rho_w(V_1 + V_2) \right] (\mu_{bed} \cos \alpha - \sin a) = \frac{U^2}{2} \rho_w C_d [(A_1 + A_2) \sin \theta + A_3 \cos \theta] \tag{10}$$

The submerged volume (V_1) of a cylindrical bole with a disk-shaped rootwad can be solved by triple integration:

$$V_1 = 2 \int_{-r}^{d_w - r} \int_{0}^{\sqrt{r^2 - y^2}} \int_{0}^{my+b} dz\, dx\, dy, \tag{11}$$

where r is the radius of the log and ($my + b$) is the equation of the water surface, with the z axis aligned parallel to log length in the center of the bole (Figure 2). Here

$$m = \frac{-1}{\tan \gamma} \tag{12}$$

and

$$b = \frac{d_w - r}{\tan \gamma} \tag{13}$$

and γ is the angle between the bole and the water surface (Figure 2) and

$$\gamma = \frac{D_{rw} - D_{\log}}{2L_{\log}} \tag{14}$$

If the water depth is greater than the piece diameter, then (11) becomes

$$V_1 = \pi\left(\frac{d_w - r}{\tan \gamma}\right) r^2. \tag{15}$$

If the water depth is less than the diameter of the log, (11) becomes

$$V_1 = \frac{2}{3 \tan (\gamma)} [r^2 - (d_w - r)^2]^{3/2} + r^2\left(\frac{d_w - r}{\tan (\gamma)}\right) \cdot \left[\sin^{-1}\left(\frac{(d_w - r)}{r}\right) + \frac{\pi}{2}\right] + \frac{1}{2} r^2\left(\frac{d_w - r}{\tan (\gamma)}\right) \sin\left[2 \sin^{-1}\left(\frac{(d_w - r)}{r}\right)\right]. \tag{16}$$

The submerged area of the bole ($A_,$) can be calculated in a similar manner:

$$A_1 = \int_{-r}^{d_w - r} \int_{0}^{my+b} dz\, dy. \tag{17}$$

If the water depth is greater than the piece diameter, then (17) becomes

$$A_1 = \frac{(d_w - r)}{\tan \gamma} r. \tag{18}$$

If the water depth is less than the diameter of the log, (17) becomes

$$A_1 = \frac{1}{2 \tan \gamma} [(d, - r)^2 - r^2] + \frac{d_w - r}{\tan \gamma} (d, - 2r). \tag{19}$$

$A_{,,}$ the submerged area of the rootwad, is

$$A_3 = 2 \int_{-D_{rw}/2}^{d_w - D_{rw}/2} \int_{0}^{(D_{rw}^2/4 - y^2)^{1/2}} dx\, dy, \tag{20}$$

where D_{rw} is the rootwad diameter. Solving the integral results in the equation

$$A_3 = \left\{2 \cos^{-1}\left(1 - \frac{2d_w}{D_{rw}}\right) - \sin\left[2 \cos^{-1}\left(1 - \frac{2d_w}{D_{rw}}\right)\right]\right\} \frac{D_{rw}^2}{8}. \tag{21}$$

The submerged volume of the rootwad (V_2) is the submerged area of the rootwad times the thickness of the rootwad (w_{rw}) assuming a disk-shaped rootwad and is equal to

$$V_2 = w_{rw}\left\{2 \cos^{-1}\left(1 - \frac{2d_w}{D_{rw}}\right) - \sin\left[2 \cos^{-1}\left(1 - \frac{2d_w}{D_{rw}}\right)\right]\right\} \frac{D_{rw}^2}{8} \tag{22}$$

The upper limit on piece movement over a smooth bed is given by a log's buoyant depth (d_b); the depth at which flotation occurs in a horizontal channel *[Braudricket al.,* 19971 is calculated by setting the gravitational force (equations (1) and (7)) equal to zero and numerically solving the equations. For pieces without rootwads the piece floats when

$$g\rho_{\log} L_{\log} \frac{\pi D_{\log}^2}{4} = g\rho_w L_{\log} A_{\text{sub}}, \tag{23}$$

where depth appears in $A_{,,,}$ (equation (6)). Pieces with rootwads float when

$$g\rho_{\log}\left(L_{\log} \frac{\pi D_{\log}^2}{4} + V_{rw}\right) = g\rho_w (V_1 + V_2), \tag{24}$$

where depth appears in V_1 and V_2 (equations (15), (16), and (24)).

Equations (4) and (10) indicate that entrainment of cylindrical pieces is a function of six piece characteristics, piece diameter, length, density, orientation with respect to flow, whether or not the piece has a rootwad, and the rootwad diameter, three channel characteristics, water depth, water velocity (a function of the depth in steady, uniform flow), and the channel slope, and two terms that are functions of both the channel and the log, the drag coefficient and the coefficient of friction between the log and the bed. Others factors such as asymmetric logs, channel shape, riparian vegetation, and obstructions such as other logs and boulders can influence the entrainment threshold of wood in streams but are not considered in these simple models, which allow us to construct simple mathematical models that we can test in the flume.

Since depth is the primary discharge-dependent variable determining entrainment, we ran numerical simulations of entrainment depth using (4) and (10) for pieces with and without simulated rootwads (i.e., attached disks) as a function of these piece and channel characteristics (Figures 3–10). We used values for some of the constituents of equations (4) and (10) that have been calculated by previous workers. *Ishikawa* [1989] found that the critical bed angle (α_{crit}, the bed angle at which the piece begins to move) is equal to 25°, which corresponds to $\mu_{\text{bed}} = 0.47$, for wood on a fine sand bed ($\mu_{\text{bed}} = \tan(\alpha_{\text{crit}})$). Velocity was calculated using Manning's equation, assuming Manning's $n = 0.013$ and channel width ($W, $) = 30 m. We assumed $\rho_{\log}$ of 500 kg m^{-3}, which is within the natural range for many tree species [*U.S. Forest Products Library,* 19761, and channel slope of 0.01, which is the slope of the channel in the flume experiments presented in this paper. Unless specifically noted, $D_{\log} = 1$ m, $L_{\log} = 15$ m, and $D,, = 2$ m, so $D_{rw}/D_{\log} = 2$.

The coefficient of drag (C,) depends on a number of factors including the orientation of the piece, the shape of the piece (whether it is a simple cylinder or had branches and/or a rootwad), the ratio of the piece length to the diameter, Froude

number, proximity to the bed, and the relative submergence of the log *[Gippelet al.,* 19961. Because C_d is dependent on a wide range of factors, we decided to use values experimentally determined by *Gippel et al.* [1996] for pieces without rootwads with a length to diameter ratio of 13:1 for the following models. In their experiment, C, was —0.9 for pieces oriented parallel to flow, 0.8 for pieces oriented at 45° to flow, and 0.9 for pieces oriented normal to flow *[Gippelet al.,* 19961. Using these values probably underestimates movement thresholds for pieces with rootwads, relative to pieces without rootwads.

Pieces oriented parallel to flow are more stable than pieces at other orientations regardless of whether or not the log has a rootwad (Figure 3). Pivoting pieces from a flow-parallel (0°) to a flow-normal (90") orientation increase the hydraulic force acting on the logs. This reduces $d_w/D_{\log}$ required for entrainment by 44% for pieces without rootwads and 31% for pieces with rootwads (Figure 3). Because of the difference in $d_w/D_{\log}$ at entrainment due solely to piece orientation, we examine the stability of each piece characteristic at 0" (flow-parallel), 45" (flow-oblique), and 90° (flow-normal) to flow.

The strongest control on piece stability is piece diameter. Doubling piece diameter increases the entrainment depth by up to 93% for pieces without rootwads and 84% for pieces with rootwads (Figure 4). The relationship between piece diameter and entrainment depth is nearly linear for pieces with and without rootwads. Increasing piece diameter of pieces without rootwads increases the differential in entrainment depths between pieces oriented parallel to flow and pieces oriented normal and oblique to flow.

In these simulations, the ratio of piece length to channel width $(L_{\log}/w_c)$ had little or no effect on the entrainment depth of pieces oriented normal and oblique to flow regardless of whether or not the piece had a rootwad (Figure 5). Increasing piece length from 5 to 30 m, for w_c = 30 m, increased $d_w/D_{\log}$ at entrainment by 19% for pieces without disks attached and 33% for pieces with simulated rootwads. However, as piece length increases, the curve in Figure 5 flattens. The point at which the curve flattens is dependent upon the ratio of the piece length to its diameter (Figure 6). The slope of the curve in Figure 6 decreases when $L_{\log}/D_{\log}$ is greater than 15.

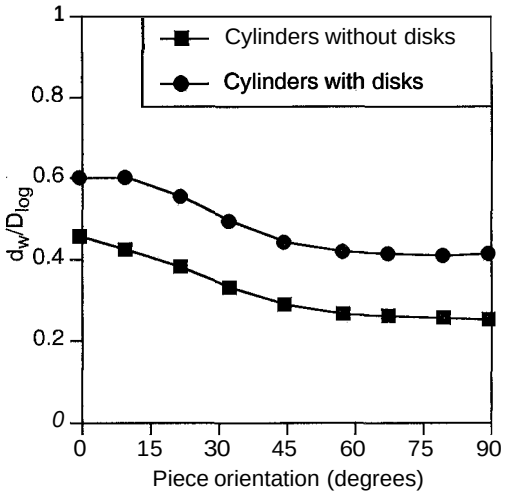

Figure 3. Theoretical plot of $d_w/D_{\log}$ at entrainment as a function of piece angle for cylinders and cylinders with simulated rootwads. $D_{\log}$ = 1m, $L_{\log}$ = 15 m, ρ_{wood} = 500 kg m^{-3}, $D_{,,}$ = 2 m, channel slope = 0.01.

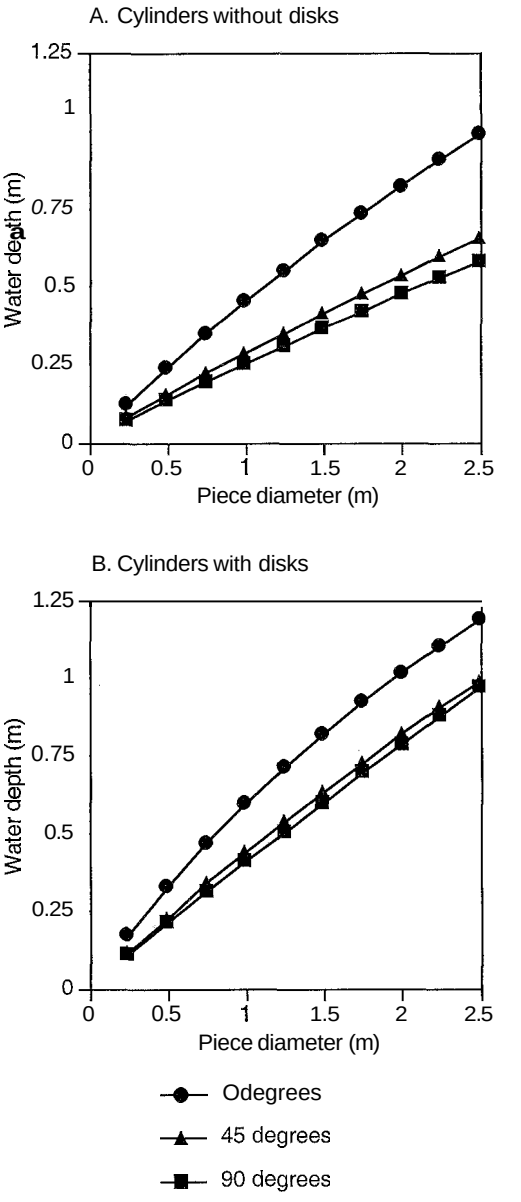

Figure 4. Theoretical plot of water depth at entrainment as a function of piece diameter for (a) cylinders and (b) cylinders with simulated rootwads. $L_{\log}$ = 15 m, ρ_{wood} = 500 kg m^{-3}, D_{rw} = 2 m, channel slope = 0.01.

The shape of the curve in Figure 5 is also dependent on the slope of the channel and the density of the log. The curves for pieces oriented parallel to flow asymptotically approach the buoyant depth (equal to 0.5 in Figure 5) for the given diameter and density as piece length increases. Piece length has little effect on entrainment of pieces without rootwads because buoyant forces are greater than drag forces, since pieces oriented parallel to flow move just prior to their flotation threshold ($d_b/D_{\log}$ = 0.5). Buoyancy is not length dependent because piece length affects buoyancy and weight (the two components of (4)) equally. In nature, the drag coefficient, C_d, might be expected to vary with piece length; however, we did not explore this dependency.

Adding a rootwad to logs increased the stability at all orientations by elevating the piece off the bed and has a greater effect on pieces oriented oblique and normal to flow than on

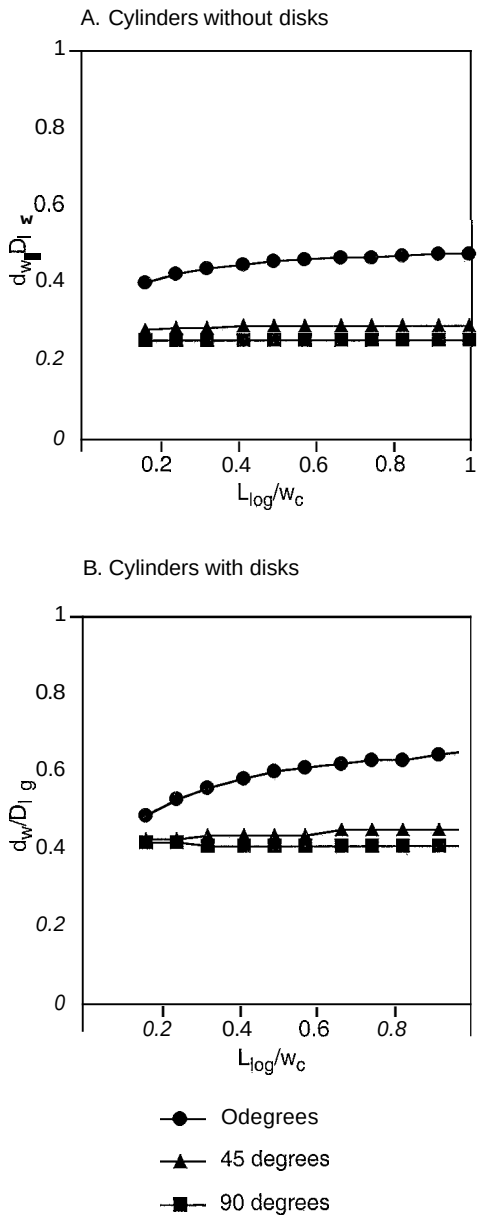

Figure 5. Theoretical plot of $d_w/D_{\log}$ at entrainment as a function of $L_{\log}/w_c$ for (a) cylinders and (b) cylinders with simulated rootwads. $D_{\log} = 1$ m, $\rho_{\text{wood}} = 500$ kg m^{-3}, $D_{,,} =$ 2 m, channel slope = 0.01.

pieces oriented parallel to flow (Figure 5). For a 15 m long log, adding a rootwad (where $D_{rw}/D_{\log} = 2$) increases the entrainment depth by 32% for pieces oriented parallel to flow and 52 and 61% for pieces oriented oblique and normal to flow, respectively. Increasing the diameter of the rootwad relative to the piece diameter reduces the buoyant force and the drag force of the log, which increases the entrainment depth regardless of orientation (Figure 7).

If a log has a rootwad, the rootwad may be more stable than the nonrootwad end of the piece, which may cause pivoting and hence torque to become an important factor in piece movement. This causes longer pieces to have a lower entrainment threshold than shorter pieces because torque is the cross product of force and the length of the lever arm. Therefore

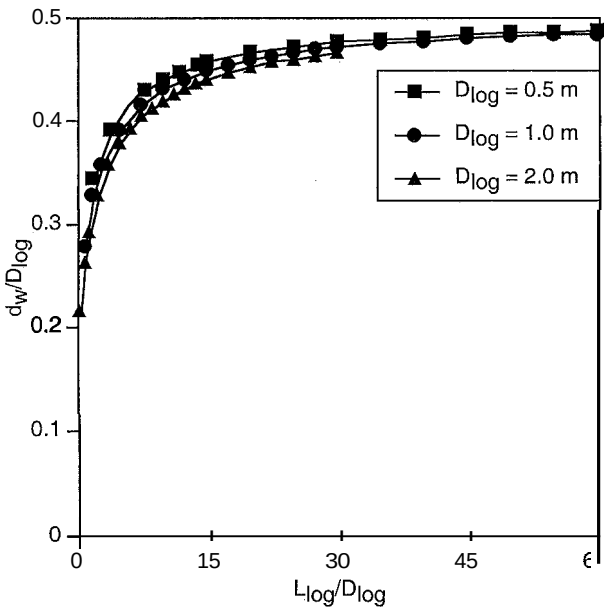

Figure 6. Theoretical plot of $d_w/D_{\log}$ at entrainment as a function of $L_{\log}/D_{\log}$ for cylinders; $\rho_{\text{wood}} = 500$ kg m^{-3}, channel slope = 0.01.

longer pieces with rootwads oriented normal and oblique to flow may move at depths below those predicted by the model.

Changing the drag coefficient (C,) has a profound effect on $d_w/D_{\log}$ at movement, particularly for pieces with simulated rootwads (Figure 8). Doubling C_d from 0.6 to 1.2 reduced $d_w/D_{\log}$ at entrainment by 6, 18, and 19% for pieces without rootwads oriented parallel, oblique, and normal to flow, respectively. The effect of an increase in C_d from 0.6 to 1.2 is much greater for pieces with rootwads, particularly those

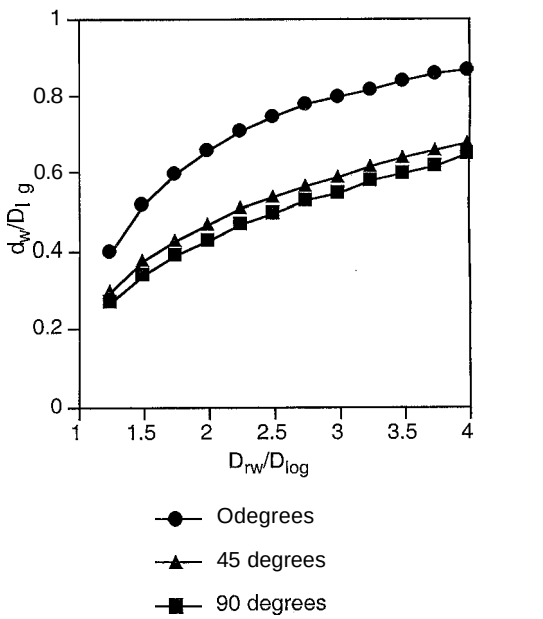

Figure 7. Theoretical plot of $d_w/D_{\log}$ at entrainment as a function of $D_{rw}/D_{\log}$ for cylinders and cylinders with simulated rootwads. $D_{\log} = 0.5$ m, $L_{\log} = 10$ m, $\rho_{\text{wood}} = 500$ kg m^{-3}, channel slope = 0.01.

oblique and normal to flow where $d_w/D_{\log}$ decreased by 53 and 52%, respectively.

Increasing slope increases the magnitude of the left-hand side of (4) and (10) but also increases the velocity for a given depth, provided that roughness does not increase. Because velocity is higher in steeper channels, the drag force is higher, which lowers the entrainment depth (Figure 9). This is particularly true for pieces oriented normal and oblique to flow because these pieces have a higher portion of their surface area exposed to flow. Increasing channel slope from 0.005 to 0.01 decreases the $d_w/D_{\log}$ required for movement by 4% for pieces without rootwads oriented parallel to flow, but by 19 and 22% for pieces without rootwads oriented oblique and normal to flow (Figure 9a). The effect on pieces with rootwads is greater than on pieces without rootwads if the piece is oriented parallel to flow but slightly less for pieces at other orientations.

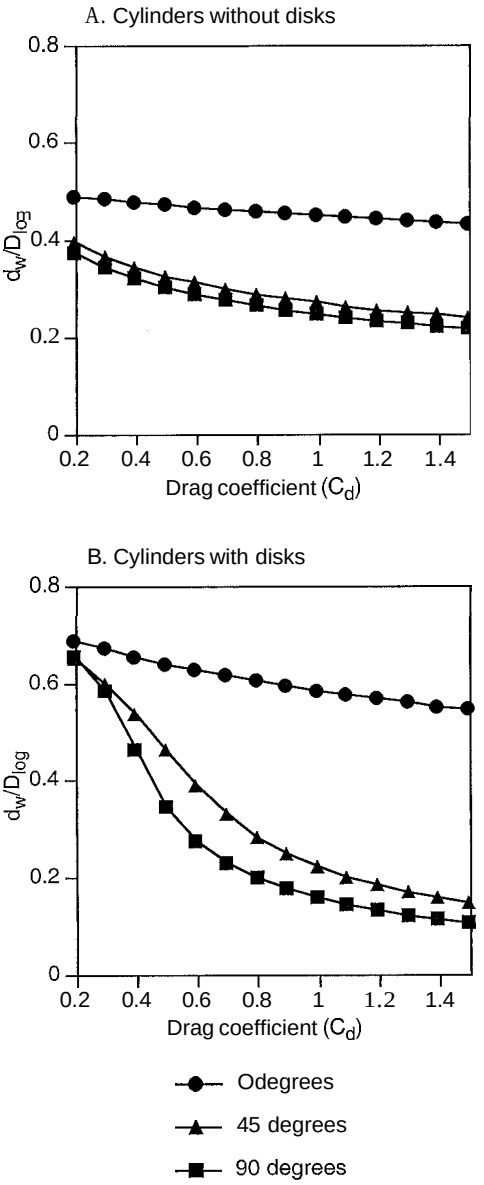

Figure 8. Theoretical plot of $d_w/D_{\log}$ at entrainment as a function of drag coefficient for (a) cylinders and (b) cylinders with simulated rootwads. $D_{\log} = 1\text{m}, L_{\log} = 15\text{m}, D_{rw} = 2$ m, $\rho_{\text{wood}} = 500$ kg m^{-3}.

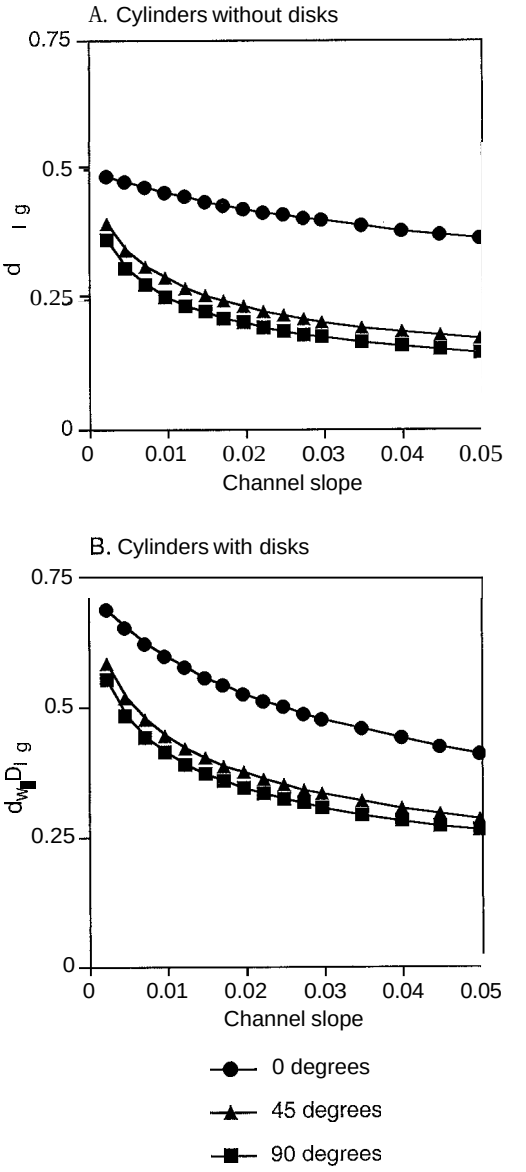

Figure 9. Theoretical plot of $d_w/D_{\log}$ at entrainment as a function of channel slope for (a) cylinders and (b) cylinders with simulated rootwads. $D_{\log} = 1\text{m}, L_{\log} = 15\text{m}, D_{,,} = 2$ m, $\rho_{\text{wood}} = 500$ kg m^{-3}.

Entrainment $d_w/D_{\log}$ is reduced by 9% for pieces oriented parallel to flow and by 16 and 17% for pieces oriented oblique and normal to flow, respectively (Figure 9b).

Increasing piece density increases the water depth relative to piece diameter required for entrainment (Figure 10). The effect on pieces without rootwads is greater than the effect on pieces with rootwads, and the effect is greater on pieces oriented parallel to flow then on pieces oriented normal and oblique to flow. Increasing log density from 300 to 700 kg m^{-3}, typical ranges for woody debris in streams, increased the $d_w/D_{\log}$ at movement by 79% for pieces without rootwads but only 42% for pieces with rootwads both oriented parallel to flow.

4. Experimental Methods

We tested these numerical models in a series of flume experiments, conducted at the University of Minnesota's St. An-

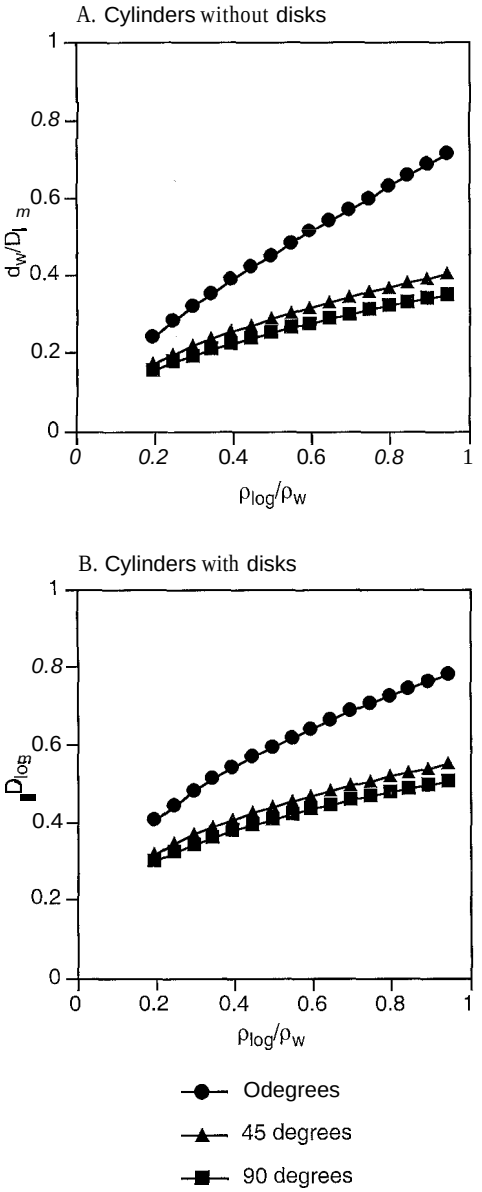

Figure 10. Theoretical plot of $d_w/D_{\log}$ at entrainment as a function of piece density for (a) cylinders and (b) cylinders with simulated rootwads. $D_{\log} = 0.5$ m, $L_{\log} = 15$ m, $D_{,,} = 2$ m, channel slope = 0.01.

thony Falls Hydraulic Laboratory, Minneapolis, Minneapolis. The flume was 1.22 m (4 feet) wide and 9.14 m (30 feet) long, with a uniform 5 cm thick planar bed of sediment at a fixed 1% slope. The sediment was pea gravel with D_{50} of ~8 mm and was immobile. Cylindrical wooden dowels with densities ranging from 436 to 735 kg m^{-3} were used to simulate logs. Rootwads were constructed by gluing wooden cabinet doorknobs, essentially a disk with cylindrical base, onto the end of the dowels. These experiments were scaled in order to preserve Froude number which averaged 0.96.

All depths were measured with a point gauge to the nearest hundredth of a centimeter. Surface velocity was measured using a float and stopwatch over a 5 m section around the original location of the log, and mean velocity was assumed to be 0.8 times the surface velocity [*Matthes*, 1956]. Velocity and depth were measured after the log had moved and were assumed to be approximately equal to their values in the presence of the log. The coefficient of friction between the log and the bed, μ_{bed}, was calculated by repeated measurement of the critical angle, (θ_{crit}), at which dowels slid down an inclined plane with attached sediment used in the flume experiments.

Pieces were placed in the flume at either 0" (flow parallel), 45" (flow oblique), or 90" (flow perpendicular), with the rootwad at the upstream end of the piece. The center of the dowels were placed 3 m from the top of the flume and 0.61 m from the sidewall in order to minimize wall and inflow effects. At the beginning of each experiment, the flow was set below the threshold of movement, as predicted by (4) and (7) and gradually raised until the piece moved one-half log length downstream. We then measured the velocity and depth at the initial location of the piece to evaluate the effects of piece length, diameter, and rootwads on the initiation of transport. Flow conditions were set below the entrainment threshold for sediment. Six pieces were used in these experiments, representing two length classes (0.30 and 0.60 m), two diameter classes (2.54 and 3.78 cm), and two lengths with 5.08 cm rootwads (both with log diameters of 2.54 cm but lengths of 0.30 and 0.60 m) (Table 1). For statistical purposes we repeated each experiment at least 5 times.

5. Results

We compared the results of our experiments (filled symbols) to the entrainment depth and velocity predicted by (4) and (10) (hollow symbols in Figures 11a–11f). Results are presented in dimensionless form to give general significance beyond the flume. In order to predict values of depth and velocity at movement, we needed values for the coefficient of friction, drag coefficient, and Manning's n. The mean $\theta_{crit} = 31.3°$ calculated using an inclined plane ($n = 20$, variance = 6.5) which corresponds to μ_{bed} equal to 0.60. We used the same drag coefficients presented by *Gippel et al.* [1996] that were used in the theoretical modeling section ($C_d = 1.05$, 0.8, and 1.0 for pieces oriented at 0°, 45°, and 90° to flow, respectively). Manning's n was assumed to be equal to 0.017, the mean value

Table 1. Experimental Conditions for Entrainment Experiments

Run	Angle, deg	Length, m	Length Class	Diameter, cm	Diameter Class	Rootwad Diameter, cm
1	0	0.3	1	2.54	1	NA
2	45	0.3	1	2.54	1	NA
3	90	0.3	1	2.54	1	NA
4	0	0.6	2	2.54	1	NA
5	45	0.6	2	2.54	1	NA
6	90	0.6	2	2.54	1	NA
7	0	0.3	1	3.81	2	NA
8	45	0.3	1	3.81	2	NA
9	90	0.3	1	3.81	2	NA
10	0	0.6	2	3.81	2	NA
11	45	0.6	2	3.81	2	NA
12	90	0.6	2	3.81	2	NA
13	0	0.3	1	2.54	1	5.08
14	45	0.3	1	2.54	1	5.08
15	90	0.3	1	2.54	1	5.08
16	0	0.6	2	2.54	1	5.08
17	45	0.6	2	2.54	1	5.08
18	90	0.6	2	2.54	1	5.08

NA, not applicable.

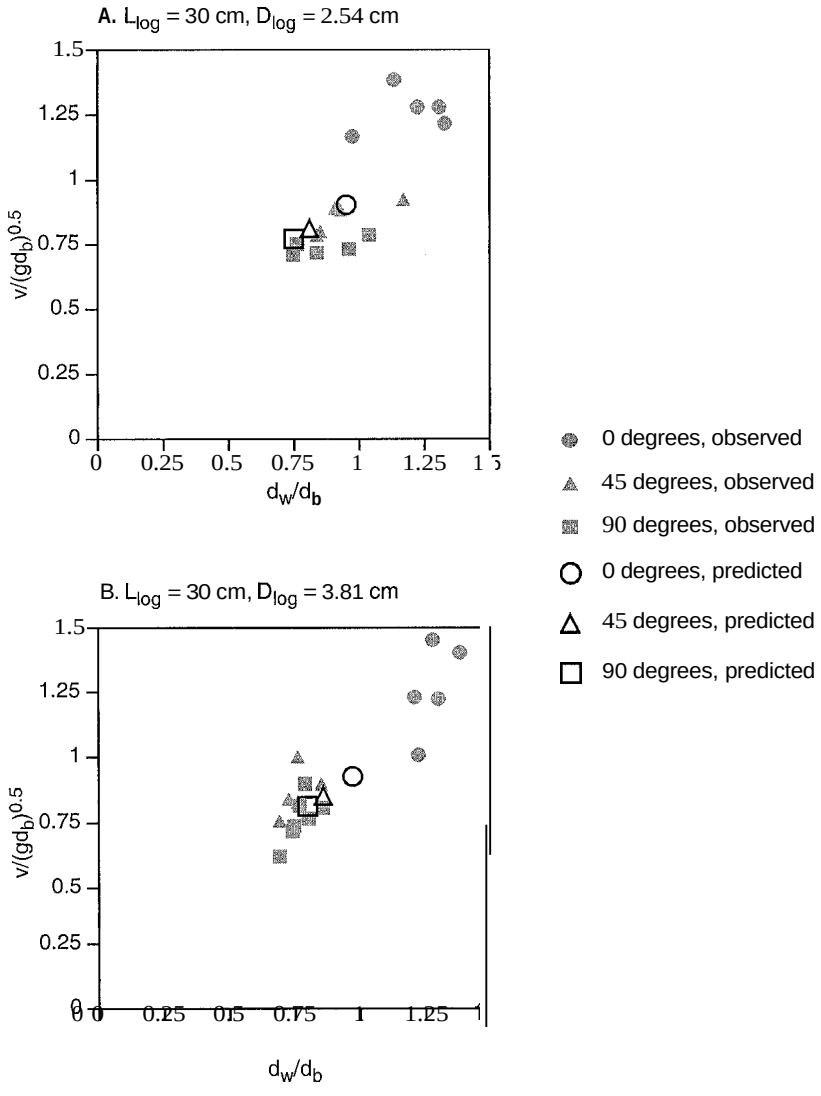

Figure 11. Observed (solid symbols) and predicted values (open symbols) of d_w/d_b and $v/(gd_b)^{0.5}$ for pieces used in the flume experiments.

calculated for these experiments. The drag coefficients are probably not accurate for our experimental conditions; however, reducing or increasing drag coefficients by 50% altered d_w/d_b by <10%, which is only slightly greater than symbol size on Figure 11.

As our model predicts, logs oriented at 0" are more stable than pieces oriented at 45° and 90°, for all lengths and diameters, regardless of whether or not they had a rootwad (Figures 11a–11f). Pieces without rootwads oriented oblique to flow (45" and 90") tend to move at depths less than their buoyant depth (Figures 11a–11d). Pieces in the larger diameter class (diameter class 2, Figures 11b and 11d) oriented normal and oblique to flow generally moved at depths less than their predicted value, whereas pieces in the smaller diameter class (diameter class 1, Figures 11a and 11c) tended to move at depths greater than their predicted values, but both diameter classes moved with 20% of predicted depths (Table 2). Pieces without rootwads oriented parallel to flow moved at depths much greater than predicted and generally 20% higher than their buoyant depths (Figures 11a–11d, Table 2); we discuss reasons for this below.

Pieces with rootwads moved at depths both greater and less than predicted (Table 2, Figures 11e–11f). However, the rootwad model seemed to be more accurate than the model for nonrootwad pieces, with most pieces oriented oblique and normal to flow moving within 10% of their predicted value (Figure 11, Table 2). Pieces oriented normal to flow in length class 2 moved at depths much less than predicted. The high variability is probably due to irregular roughness elements on the bed. In general, we were relatively successful at predicting depths of movement for pieces oriented at 45° and 90" but again underestimated the stability of pieces oriented parallel to flow.

Although not considered by the model, we observed pivoting to be an important process initiating motion for all pieces but particularly for those oriented at 45° and 90". Pieces without rootwads oriented at 45° and 90" tended to pivot and roll toward 0" while moving down the flume, often as the first stage of movement. Pieces oriented at 0" tended to float at either end, pivot slightly, and roll downstream. Pivoting was also very important for pieces with rootwads, particularly those oriented at 45" and 90°. These pieces rolled downstream, pivoted toward

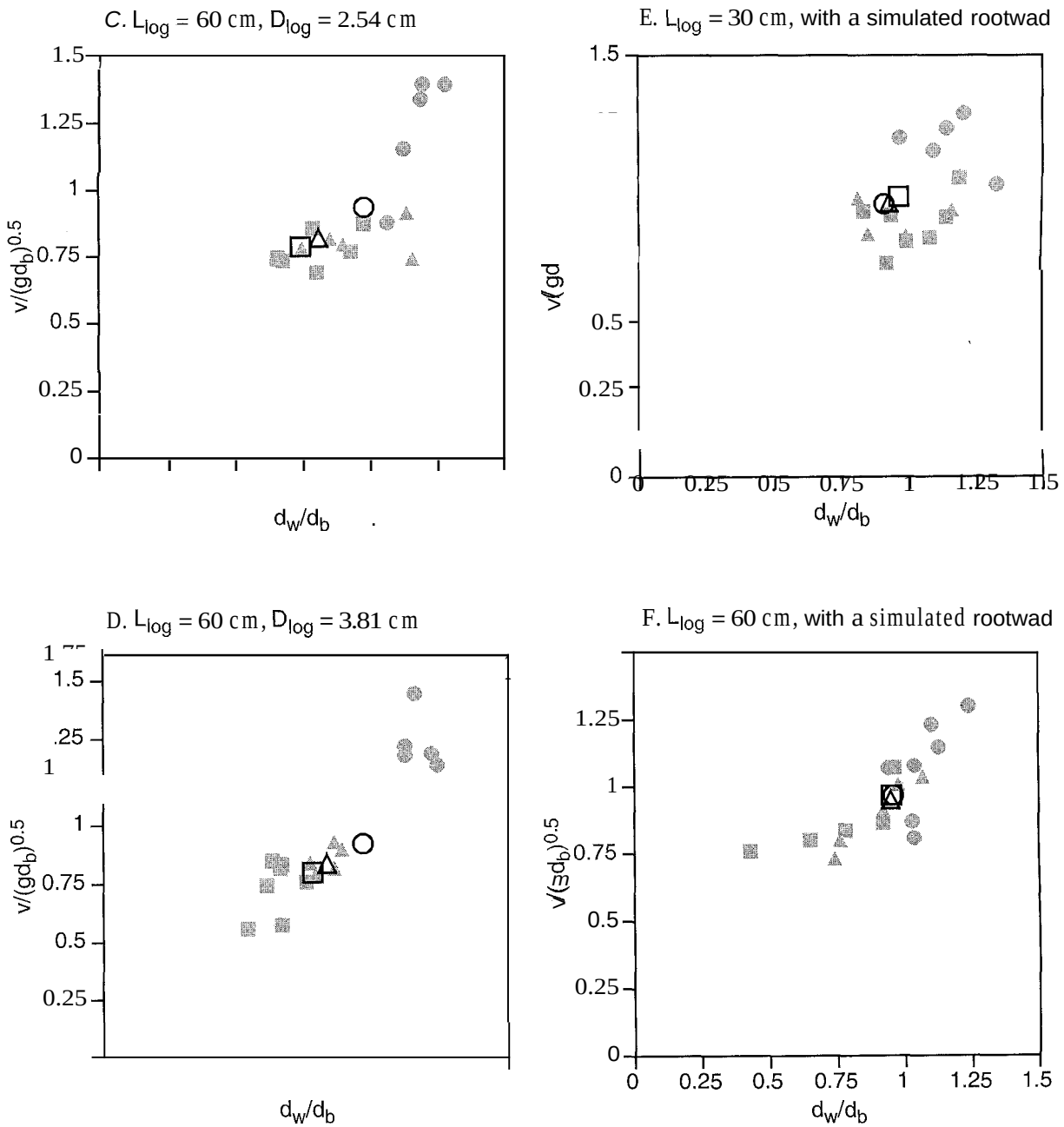

Figure 11. (continued)

0°, and stabilized just downstream of their initial location. Under flow conditions observed, stability of pieces with rootwads was essentially controlled by their stability at 0°, since this is where motion effectively ceased. Movement of rootwad pieces initially oriented at 0" began with flotation of the nonrootwad end, then the rootwad would move forward while dragging along the bed. We believe that the increased propensity of longer logs with rootwads to pivot due to torque allowed pieces oriented at 90° to move downstream at depths and velocities below those predicted.

The increased stability of pieces oriented parallel to flow is due either to resistance offered by gravel particles just downstream of the piece that obstructed movement or to deflation of the water surface elevation caused by deflection of flow around the upstream end of the piece. We performed one experiment where we removed the gravel from just downstream of the piece, and the piece moved, leading us to believe that grain roughness increases stability of pieces oriented parallel to flow. The tendency of pieces oriented parallel to flow to float at one end and pivot slightly before moving implies that the piece was held in place by downstream coarse sediment. Because this resistance varies depending on the size and numbers of particles downstream of the piece it is difficult to assess its value, but future experiments need to consider the grain size distribution of the bed as an additional factor.

6. Discussion

Movement of wood in streams is far more complex than movement of sediment. The combination of a cylindrical bole

Table 2. Results of Entrainment Experiments

Run	Length Class	Diameter Class	Rootwad	Angle, deg	d_{mean}, cm	d_{pred}, cm	d_b, cm	d_{mean}/d_{pred}	d_{mean}/d_b
1	1	1	no	0	1.87	1.41	1.55	1.33	1.34
2	1	1	no	45	1.47	1.28	1.55	1.15	0.95
3	1	1	no	90	1.36	1.18	1.55	1.16	0.88
4	2	1	no	0	2.05	1.72	1.73	1.19	1.22
5	2	1	no	45	1.68	1.42	1.73	1.18	0.97
6	2	1	no	90	1.34	1.30	1.73	1.03	0.80
7	1	2	no	0	2.14	1.63	1.66	1.31	1.29
8	1	2	no	45	1.28	1.45	1.66	0.89	0.77
9	1	2	no	90	1.30	1.35	1.66	0.96	0.78
10	2	2	no	0	2.17	1.77	1.83	1.23	1.35
11	2	2	no	45	1.52	1.54	1.83	0.99	0.83
12	2	2	no	90	1.18	1.43	1.83	0.83	0.65
13	1	1	yes	0	2.50	2.03	2.14	1.23	1.17
14	1	1	yes	45	2.17	2.05	2.14	1.06	1.01
15	1	1	yes	90	2.20	2.10	2.14	1.05	1.03
16	2	1	yes	0	2.21	1.96	2.04	1.13	1.08
17	2	1	yes	45	1.84	1.98	2.04	0.93	0.90
18	2	1	yes	90	1.54	1.99	2.04	0.78	0.75

Here d_b is the buoyant depth, d_{mean} is the mean measured flow depth at entrainment, and d_{pred} is the predicted entrainment depth.

attached to an irregular rootwad, large size relative to channel dimensions, and opportunity for various orientations relative to flow contribute to larger number of variables needing to be considered in predicting entrainment, even in simple, immobile bed channels. In predicting wood movement, unequal forces exerted on different parts of the log, including effects of flotation, need to be considered. Moreover, different types of wood movement are possible, including sliding, rolling, pivoting, and floating.

The simple force balance model developed here considers only some of these factors. We present the simplest case of initiation of movement by sliding of geometrically regular pieces over an immobile bed with steady uniform flow. Although our theoretical models (equations (4) and (10)) assume that pieces begin to move by sliding, we observed both rolling and pivoting movement in our experiments, particularly where pieces were oriented oblique or normal to flow. Despite this, our model predicted incipient motion for oblique or normal orientations relatively well for pieces without rootwads; generally, predicted movement depths were within 20% of observed values (Table 2). We infer that the movement threshold for sliding must therefore be relatively close to that for pivoting or rolling for these orientations, assuming that our drag coefficients are correct.

The model performed less adequately in predicting movement for pieces oriented parallel to flow, those that would be most expected to move by sliding. **A** confounding factor, however, was the presence of large grain roughness in our experimental runs that limited downstream movement of logs lodged against protruding bed particles. Further experiments with a smoother bed may help reduce the scatter between predicted and observed depths for flow-parallel pieces.

Field studies indicate that piece length is a first-order control on piece stability [e.g., *Nakamura and Swanson*, 1994; *Abbe and Montgomery*, 1996]. Theory and these experiments, however, indicate that piece length only influences pieces oriented parallel to flow for piece size used in the modeling and experiments. Although we saw little influence of diameter on piece entrainment because significant density differences between pieces in diameter class 1 and class 2 made their buoyant depths approximately equal (Table 2), diameter strongly influences entrainment depth in theory (Figure 4).

There are several factors that can account for the difference between results of previous field studies on entrainment that highlighted piece length as a key factor and our experiments. First, many previous studies occurred on small streams where logs are typically much longer than channel width and bed roughness is high. In these small channels, longer pieces may be completely or partially suspended over the channel and therefore less likely to be in contact with the flow; consequently (4) and (10) cannot be used. Both our force-balance model and these experiments use simplified geometries to model pieces. However, because trees often break into pieces upon impact [*Van Sickle and Gregoy*, 1990], cylinders are a reasonable model for many logs in streams. Rootwads typically tend to have an irregular shape with an open framework, which decreases the drag force acting on the piece, relative to the disks used in our experiments. Riparian vegetation can also play an important role in piece stability. Long pieces are more likely to be lodged upstream of riparian trees or other obstructions that increase piece stability. Scour holes can also form around rootwads in the field, which serve to further increase the stability of pieces with rootwads. We did not model any of these conditions in our entrainment experiments, all of which would tend to increase the stability of logs in streams. Equations (4) and (10) and these experiments best represent minimum thresholds for movement.

Dimensional analysis of our experimental conditions (Table 3) indicates that these flume experiments best represent entrainment of pieces in large rivers and unconstrained reaches of medium sized streams. In these streams, where piece length is typically less than channel width, pieces tend to lodge on and be entrained from streamside bars, floodplains, and midchannel bars. On such surfaces, inundation depths are typically rather uniform across the bar relative to smaller channels, and suspension of pieces is rare. Sediment was unusually coarse in our experiments in order to maintain an immobile bed (D_{50} = 0.008 m) which corresponds to a field D_{50} of 0.315 m or a cobble-bed stream. The interaction between pieces and grain

Table 3. Dimensional Analysis of Experimental Variables

Characteristic	Experimental Conditions	Corresponding Field Conditions	Typical Ranges in Pool-Bar Forested Streams
Piece length	0.3–0.6 m	11.8–23.6 m	2–30 m
Piece diameter	0.0254–0.0381 m	1–1.5 m	0.25–2.0 m
Rootwad diameter	0.0508 m	2 m	0.5–3.0 m
Water depth	0.018 m	0.71 m	0.5–5
Channel width	1.21 m	39.3 m	20–100 m
Grain size	0.008 m	0.315 m	finer
Froude number	0.96	0.96	0.5–1.5
Reynolds number	7341	7341	>10,000
Channel slope	0.01	0.01	0.005–0.025
Wood density	435–736 kg m^{-3}	435–736 kg m^{-3}	300–700 kg m^{-3}
Manning's n	0.017	0.017	0.02–0.05

Defining the smallest diameter used as 1 m gives a scaling factor of 39.4. Values of wood density were obtained from *U.S. Forest Products Laboratory* [1976].

roughness was a significant factor in determining when pieces moved and where they lodged.

Diameter is the most important factor determining piece stability, from a management perspective provided that piece length is less than channel width. Orienting pieces parallel to flow, or using pieces with rootwads will increase the stability of pieces added by at least 39 and 71%, respectively. However, because fluvially deposited pieces tend to be oriented parallel to flow *[Nakamura and Swanson*, 1994], diameter and the presence of rootwads are the most important piece characteristics when determining piece stability. Entrainment curves for pieces of various densities and geometries can be constructed using (4) and (10), which can then be used to assess piece stability, assuming initial movement is from sliding.

Other channel characteristics which were not included in either our theoretical model or our experiments can have a profound effect on piece stability. Pieces added to streams in areas with riparian vegetation and other roughness elements may be more stable than shown here. Any management practice that decreases the roughness or removes riparian vegetation (making streams look like our flume) will reduce the stability of longer pieces, which are often the key pieces in jam formation. Although our model does not account for obstructions and suspension of pieces over the channel, each of these factors increases the flow depth required for entrainment. Our model therefore can be used as a first-order minimum estimate for flows at which in-channel pieces will be stable and as a model to predict the stability of pieces added to streams. Future work should incorporate other types of initial movement (rolling, pivoting) as well as explicitly addressing the effects of bed and bank roughness on movement.

7. Conclusions

A force balance model and these experiments show that the two most important factors in the entrainment of pieces are the piece orientation and the presence/absence of rootwads. The data plotted into two groups where pieces without rootwads oriented at 0" to flow and pieces with rootwads were the most stable and moved after their flotation threshold, and pieces without rootwads oriented at 45" and 90° to flow were the least stable and moved below their flotation threshold mostly by pivoting into a flow parallel position. Pieces with rootwads oriented parallel to flow were more stable than pieces with rootwads oriented at 45° and 90° to flow. However, pieces with rootwads oriented at 45° and 90° to flow pivoted toward 0" and did not move far, indicating that the stability of pieces with rootwads oriented at 45° and 90° is essentially the same as pieces oriented at 0". Although previously reported as the most important factor determining piece stability, both the experiments and force balance model show that piece length does not play a significant role in determining piece stability because buoyant forces dominate drag forces.

We believe that field results showing that longer pieces are more stable than shorter pieces are partly because most studies have occurred in relatively small channels where long pieces can either be suspended over the channel or have much of their length outside the channel. In addition, longer pieces are more likely to be lodged upstream of obstructions such as riparian vegetation and boulders. Under uniform depth, there is no physical reason why longer pieces should be more stable than shorter pieces.

Our theoretical model reasonably predicted entrainment thresholds for pieces oriented at 45" and 90" to flow but underestimated the flows at which pieces oriented parallel to flow moved. We believe this is due to resistance provided by sediment grains on the downstream end of the piece and is an artifact of the coarse grain size used in these experiments. However, bed roughness may be a factor in real streams as well. Both the physical model and these experiments best model wood in large streams, where the depth is uniform across the cross section.

Notation

A_1 submerged area of the bole for pieces with rootwads.
A_2 submerged area of the rootwad, perpendicular to piece length.
A_3 submerged area of the rootwad, parallel to piece length.
A_{sub} submerged log area for logs without rootwads.
C_d drag coefficient between the log and the water.
d_b buoyant depth of the log.
D_{log} log diameter.
D_{rw} rootwad diameter.
d_w water depth.
F_{drag} drag force acting on the log.
$F_{friction}$ frictional force acting on the log.
$F_{gravity}$ gravitational force acting on the log (in the downstream direction).
F_n normal force acting on the log.

g acceleration due to gravity.
$L_{\log}$ log length.
r log radius.
U water velocity.
V_1 submerged volume of the bole, for logs with rootwads.
V_2 submerged rootwad volume.
V_{rw} rootwad volume.
w, channel width.
W_{eff} effective weight of a log.
w_{rw} rootwad width assuming a disk-shaped rootwad.
α bed slope.
α_{crit} critical bed slope at which sliding occurs without drag.
γ angle between the bole and the water surface (see (6)).
μ_{bed} coefficient of friction between the log and the bed.
$\rho_{\log}$ log density.
ρ_w water density.
θ piece orientation with respect to flow, 0° is parallel to flow, and 90" is perpendicular to flow.
$m = -1/\tan \gamma$.
$b = (d_w - r)/\tan \gamma$.

Acknowledgments. This research was funded by grants from the Ecosystem processes program of the Pacific Northwest Research Station, the Coastal Landscape Analysis and Modeling Project, and the National Science Foundation Long Term Ecological Research Network Grant to the H. J. Andrews Experimental Forest (LTER3-BSR8514325). Initial discussions with Dave Montgomery and Tim Abbe helped frame the problem of wood entrainment in streams. We would like to thank everyone at the St. Anthony Falls Hydraulic Laboratory for assistance with these experiments. In particular, we would like to thank Gary Parker, Jasim Imran, Carlos Toro-Escobar, Scott Morgan, Richard Voight, and Benjamin Erickson for their assistance, advice, and encouragement. In-house reviews by Stephen Lancaster, Fred Swanson, and Julia Jones were very helpful. We would also like to thank Tom Lisle, Dave Montgomery, Jim Pizutto, and Matt O'Connor for their reviews of this manuscript for *Water Resources Research.* Mathematical assistance was provided by David Phlean.

References

Abbe, T. B., D. R. Montgomery, K. Featherston, and E. McClure, A process-based classification of woody debris in a fluvial network; Preliminary analysis of the Queets River, Washington, *Eos Trans. AGU, 74*(43), Fall Meet. Suppl., F296, 1993.

Abbe, T. B., and D. R. Montgomery, Large woody debris jams, channel hydraulics and habitat formation in large rivers, *Reg. Rivers Res. Manage.,* 12, 201–221, 1996.

Abbe, T. B., D. R. Montgomerey, G. Pess, T. Drury, and C. Petroff, Emulating organized chaos: Engineered log jams as a tool for rehabilitating fluvial environments, *Eos Trans. AGU, 79*(46), Fall Meet. Suppl., F345–F346, 1998.

Bilby, R. E., Influence on stream size on the function and characteristics of large organic debris, paper presented at West Coast Meeting of the National Council of the Paper Industry for Air and Stream Improvement, Nat. Counc. for the Pap. Ind., Portland, Oreg., 1985.

Bilby, R. E., and J. W. Ward, Changes in characteristics and function of large woody debris with increasing size of streams in western Washington, *Trans. Am. Fish. Soc.*, 118, 368–378, 1989,

Bilby, R. E., and J. W. Ward, Changes in characteristics and function of large woody debris in streams draining old-growth: Clear-cut, and second-growth forests in southwestern Washington, *Can. J. Fish. Aquat. Sci.,* 48, 2499–2508, 1991.

Braudrick, C. A., G. E. Grant, Y. Ishikawa, and H. Ikeda, Dynamics of wood transport in streams: A flume experiment, *Earth Surf. Processes Landforms*, 22, 669–683, 1997.

Gippel, C. J., I. C. O'Neil, B. L. Finlayson, and I. Scnatz, Hydraulic guidelines for the reintroduction and management of large woody debris in lowland rivers, *Reg. Rivers Res. Manage.,* 12,223–236, 1996.

Gregory, S. V., Spatial and temporal patterns of woody debris retention and transport, *Bull. N. Am. Benthological Soc., 8,* 15, 1991.

Harmon, M. E., et al., Ecology of coarse woody debris in temperate ecosystems,*Adv. Ecol. Res.,* 15, 133–302, 1986.

Hogan, D. L., The influence of large organic debris on channel recovery in the Queen Charlotte Islands, British Columbia, Canada, paper presented at Corvallis Symposium: Erosion and Sedimentation in the Pacific Rim, Int. Assoc. of Hydrol. Sci., Corvallis, Oreg., 1987.

Ishikawa, Y., Studies on disasters caused by debris flows carrying floating logs down mountain streams, Ph.D. thesis, 121 pp., Kyoto University, Kyoto, Japan, 1989.

Lienkaemper, G. W., and F. J. Swanson, Dynamics of large woody debris in old-growth Douglas-fir forests, *Can. J. For. Res.,* 17, 150–156, 1987.

Lisle, T. E., Effects of coarse woody debris and its removal on a channel effected by the 1980 eruption of Mount St. Helens, Washington, *Water Resour. Res., 31,* 1797–1808, 1995.

Matthes, G., River surveys in unmapped territory, *Trans. Am. Soc. Civ. Eng.*, 121,739–758, 1956.

Montgomery, D. R., T. B. Abbe, J. M. Buffington, N. P. Peterson, K. M. Schmidt, and J. D. Stock, Distribution of bedrock and alluvial channels in forested mountain drainage basins, *Nature,* 381, 587–589, 1996.

Nakamura, F., and F. J. Swanson, Distribution of coarse woody debris in a mountain stream, western Cascades Range, Oregon, *Can. J. For. Res.,* 24, 2395–2403, 1994.

Sedell, J. R., and J. L. Froggatt, Importance of streamside forests to large rivers: The isolation of the Willamette River, Oregon, U.S.A., from its floodplain by snagging and streamside forest removal, *Int. Assoc. TheoreticalAppl. Limnol.,* 22, 1828–1834, 1984.

Toews, D. A. **A.,** and M. K. Moore, The effects of three streamside logging treatments on organic debris and channel morphology in Carnation Creek, paper presented at Carnation Creek Workshop, Malaspina College, Naniamo, B. C.,, 1982.

U.S. Forest Products Library, *Wood Handbook: Wood as an Engineering Material, USDA Agric. Handbook* 72, U.S. Dep. of Agric., Madison, Wisc., 1976.

Van Sickle, J., and S. V. Gregory, Modeling inputs of large woody debris to streams from falling trees, *Can. J. For. Res.,* 20, 1593–1601, 1990.

Young, M. K., Movement and characteristics of stream-bourne coarse woody debris in adjacent burned and undisturbed watersheds in Wyoming, *Can. J. For. Res.,* 24, 1933–1938, 1994.

C. A. Braudrick, Department of Geosciences, Oregon State University, Corvallis, OR 97333. (cbraudrick@hotmail.com)

G. E. Grant, Pacific Northwest Research Station, U.S. Forest Service, Corvallis, OR 97333.

(Received April 23, 1999; revised September 20, 1999;
accepted September 21, 1999.)